Benchmark on Adaptive Regulation - Rejection of unknown/time-varying multiple narrow band disturbances

Ioan Doré Landau*, Abraham Castellanos Silva*, Tudor-Bogdan Airimitoaie*, Gabriel Buche*, Mathieu Noe†

Abstract—**The adaptive regulation is an important issue with a lot of potential for applications in active suspension, active vibration control, disc drives control and active noise control. One of the basic problems from the "control system" point of view is the rejection of multiple unknown and time varying narrow band disturbances without using an additional transducer for getting information upon the disturbances. An adaptive feedback approach has to be considered for this problem. Industry needs a *state of the art* in the field based on a solid experimental verification on a system using a current used technology. The paper presents a benchmark problem for suppression of multiple unknown and/or time-varying vibrations and an associated active vibration control system using an inertial actuator on which the experimental verifications have been done. The objective is to minimize the residual force by applying an appropriate control effort through the inertial actuator. The system does not use any additional transducer for getting in real-time information upon the disturbances.**

The benchmark has three levels of difficulty and the associated control performance specifications are presented. A simulator of the system has been used by the various contributors to the benchmark to test their methodology. The procedure for real-time experiments is briefly described [1]. The performance measurement methods used will be presented as well as an extensive comparison of the results obtained by various approaches[2].

Index Terms—**Adaptive Regulation, Active Vibration Control, Inertial Actuators, Multiple Narrow Band Disturbances, Youla-Kučera Parametrization, Internal Model Principle**

I. Introduction

One of the basic problems in control is the attenuation (rejection) of unknown disturbances without measuring them. The common framework is the assumption that the disturbance is the result of a white noise or a Dirac impulse passed through the *model of the disturbance*. The knowledge of this model allows to design an appropriate controller. When considering the model of a disturbance, one has to address two issues: 1) its structure (complexity, order of the parametric model) and 2) the values of the parameters of the model. In general, one can assess from data the structure for such *model of disturbance* (using spectral analysis or order estimation techniques) and assume that the structure does not change. However the parameters of the model are unknown and may be time varying. This will require to use an adaptive feedback approach.

*Control system department of GIPSA-LAB, St. Martin d'héres, 38402 FRANCE (e-mail: [ioan-dore.landau, tudor-bogdan.airimitoaie, abraham.castellanos-silva, Gabriel.Buche]@gipsa-lab.grenoble-inp.fr).

† Paulstra S.A.; Vibrachoc Division

[1]The GIPSA-LAB team has done the experiments for all the contributors.

[2]Simulation and Real-time results are presented by each contributor in their papers [4], [8], [13], [25], [6], [1], [23].

The classical adaptive control paradigm deals essentially with the construction of a control law when the parameters of the plant dynamic model are unknown and time varying ([20]). However, in the present context, the plant dynamic model is almost invariant and it can be identified and the objective is the rejection of disturbances characterized by unknown and time varying disturbance models. It seems reasonable to call this paradigm *adaptive regulation*. In classical "adaptive control" the objective is tracking/disturbance attenuation in the presence of unknown and time varying plant model parameters. Therefore adaptive control focuses on adaptation with respect to plant model parameters variations. The model of the disturbance is assumed to be known and invariant. Only a level of attenuation in a frequency band is imposed (with the exception of DC disturbances where the controller may include an integrator). In *adaptive regulation* the objective is to asymptotically suppress (attenuate) the effect of unknown and time-varying disturbances. Therefore adaptive regulation focuses on adaptation of the controller parameters with respect to variations in the disturbance model parameters. The plant model is assumed to be known. It is also assumed that the possible small variations or uncertainties of the plant model can be handled by a robust control design. The problem of adaptive regulation as defined above has been previously addressed in a number of papers ([5], [2], [24], [22], [9], [11], [12], [19], [14], [3], [7], [10]) among others. [15] presents a survey of the various techniques (up to 2010) used in adaptive regulation as well as a review of a number of applications.

The industry needs a *state of the art* in the field based on a solid experimental verification on a benchmark. The objective of the proposed benchmark is to evaluate on an experimental basis the available techniques for adaptive regulation in the presence of unknown/time varying multiple narrow band disturbances. Active vibration control constitutes an excellent example of a field where this situation occurs. But similar situations occur in disc drives control and active noise control. Solutions for this problem in active vibration control can be extrapolated to the control of disc drives and active noise control (see for example the applications described in [15]). The benchmark will effectively test various approaches in the specific context of an active vibration control system which will be used as a test bed.

The scientific objective of the benchmark is to evaluate current available procedures for adaptive regulation which may be applied in the presence of unknown/time varying multiple narrow band disturbances. The benchmark specifically will focus in testing: 1) performances, 2) robustness and 3) complexity.

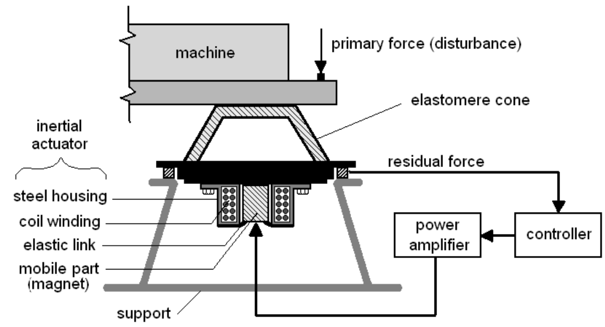

Fig. 1. Active vibration control using an inertial actuator (scheme).

The test bed is an active suspension using an inertial actuator and equipped with a shaker and a measure of the residual force. It is located at GIPSA-Lab, Grenoble (France).

The paper is organized as follows. Section II gives a description of the active vibration control system used, as well as some details upon the simulator. Section III gives the basic equations describing the system and the disturbance along with some information upon the identified models . Section IV presents the control specifications as well as the protocols used on the benchmark. Section V describes some differences found between the simulator and the real plant and how these were taken into account. A methodological comparison of the various approaches is made in Section VI. The description of the measurements used for the analysis is done in Section VII. Section VIII gives the evaluation criteria defined with respect to the benchmark specifications as well as a comparison of obtained results. The complexity evaluation is done in Section IX and the performance robustness with respect to experimental protocol changes is analyzed in Section X. The main conclusions for this benchmark are given in Section XI. Appendix XII presents a comparison of the adaptation algorithms used by the various contributors.

II. An active vibration control system using an inertial actuator

A. System structure

The structure of the system used for the benchmark is presented in figure 1. A general view of the whole system including the testing equipment is shown figure 2. It consists of a passive damper, an inertial actuator, a load, a transducer for the residual force, a controller, a power amplifier and a shaker. The mechanical construction of the load is such that the vibrations produced by the shaker, fixed to the ground, are transmitted to the upper side, on top of the passive damper. The inertial actuator will create vibrational forces which can counteract the effect of vibrational disturbances (inertial actuators use a similar principle as loudspeakers). It is fixed to the chassis where the vibrations should be attenuated. The controller, through the power amplifier, will generate current in the mobile coil which will produce a movement in order to reduce the residual force. The equivalent control scheme is shown in figure 3. The system input, $u(t)$ is the

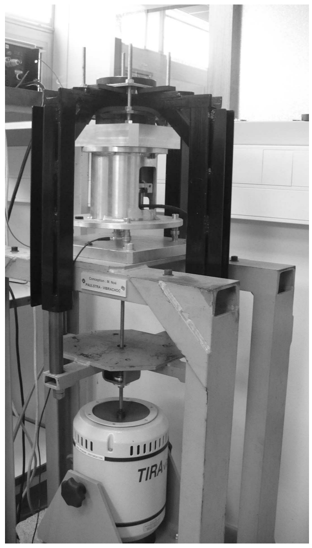

Fig. 2. Active vibration control system (photo).

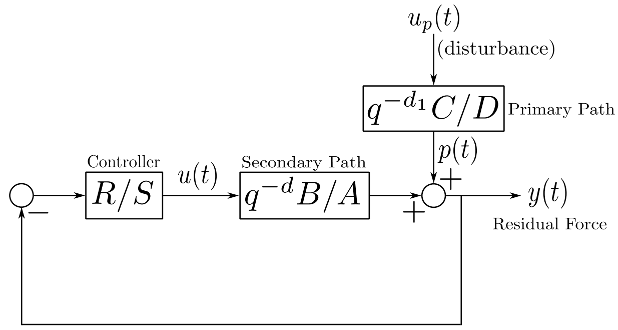

Fig. 3. Block diagram of active vibration control systems.

position of the mobile part (magnet) of the inertial actuator (see figures 1, 3 and 4), the output $y(t)$ is the residual force measured by a force sensor. The transfer function ($q^{-d_1}\frac{C}{D}$), between the disturbance force, $u_p(t)$, and the residual force $y(t)$ is called *primary path*. In our case (for testing purposes), the primary force is generated by a shaker driven by a signal delivered by the computer. The plant transfer function ($q^{-d}\frac{B}{A}$) between the input of the inertial actuator, $u(t)$, and the residual force is called *secondary path*. Since the input of the system is a position and the output a force, the secondary path transfer function has a double differentiator behavior.

The control objective is to reject the effect of unknown narrow band disturbances on the output of the system (residual force), i.e. to attenuate the vibrations transmitted from the machine to the chassis. The physical parameters of the system are not available. The system has to be considered as a *black box* and the corresponding models for control design should be identified. The sampling frequency is $F_s = 800$ Hz.

The block diagram of the active vibration control system emphasizing the hardware aspects is shown in figure 4.

Data used for system identification as well as the models identified from these data by the organizers are available on the benchmark website (http://www.gipsa-lab.grenoble-inp.fr/~ioandore.landau/ benchmark_adaptive_regulation/index.html).

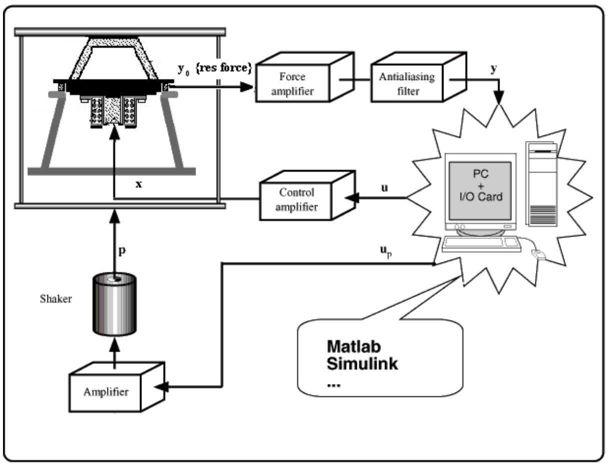

Fig. 4. The active vibration control system - hardware configuration.

B. Simulator

A ***black box*** discrete time simulator of the active suspension built on MATLAB©Simulink (2007 version) has been provided (can be downloaded from the benchmark website). It uses the models identified by the organizers.

The control scheme (*Controller*) should be built around the given simulator. The simulator has been used by the participants to the benchmark to set the appropriate control scheme and test the performance.

C. Real time implementation

The real time implementation uses the MATLAB xPC Target environment (2007). The PC for program development is a Dell©Optiplex 760. The PC target (Dell Optiplex GX270 with Pentium©4 at 2.86 GHz) is equipped with I/O data acquisition board, A/D and D/A converters. The procedure compiles the algorithms directly from the Simulink scheme provided by the participants. The experiments on the benchmark test bed (for all the contributions) have been done by the organizers of the benchmark. More details on the system, the data acquisition and the simulator can be found on the benchmark website: http://www.gipsa-lab.grenoble-inp.fr/~ioandore.landau/benchmark_adaptive_regulation/index.html.

III. Plant/disturbance representation and controller structure

The structure of the linear time invariant discrete time model of the plant - the secondary path - used for controller design is:

$$G(z^{-1}) = \frac{z^{-d}B(z^{-1})}{A(z^{-1})} = \frac{z^{-d-1}B^*(z^{-1})}{A(z^{-1})} \ , \qquad (1)$$

with:

$d =$ the plant pure time delay in number of sampling periods

$$A = 1 + a_1 z^{-1} + \cdots + a_{n_A} z^{-n_A} \ ;$$
$$B = b_1 z^{-1} + \cdots + b_{n_B} z^{-n_B} = z^{-1}B^* \ ;$$
$$B^* = b_1 + \cdots + b_{n_B} z^{-n_B+1} \ ,$$

where $A(z^{-1})$, $B(z^{-1})$, $B^*(z^{-1})$ are polynomials in the complex variable z^{-1} and n_A, n_B and $n_B - 1$ represent their orders[3]. The model of the plant may be obtained by system identification. Details on system identification of the models considered in this paper can be found in [21], [18], [17].

Since the benchmark is focused on regulation, the controller to be designed is a *RS*-type polynomial controller (or an equivalently state space controller + observer) ([20], [21]) - see also figure 3).

The output of the plant $y(t)$ and the input $u(t)$ may be written as:

$$y(t) = \frac{q^{-d}B(q^{-1})}{A(q^{-1})} \cdot u(t) + p(t) \ ; \qquad (2)$$
$$S(q^{-1}) \cdot u(t) = -R(q^{-1}) \cdot y(t) \ , \qquad (3)$$

where q^{-1} is the delay (shift) operator ($x(t) = q^{-1}x(t+1)$) and $p(t)$ is the resulting additive disturbance on the output of the system. $R(z^{-1})$ and $S(z^{-1})$ are polynomials in z^{-1} having the orders n_R and n_S, respectively, with the following expressions:

$$R(z^{-1}) = r_0 + r_1 z^{-1} + \ldots + r_{n_R} z^{-n_R} = R'(z^{-1}) \cdot H_R(z^{-1}) \ ; \qquad (4)$$
$$S(z^{-1}) = 1 + s_1 z^{-1} + \ldots + s_{n_S} z^{-n_S} = S'(z^{-1}) \cdot H_S(z^{-1}) \ , \qquad (5)$$

where H_R and H_S are pre-specified parts of the controller (used for example to incorporate the internal model of a disturbance or to open the loop at certain frequencies).

We define the following sensitivity functions:

- Output sensitivity function (the transfer function between the disturbance $p(t)$ and the output of the system $y(t)$):

$$S_{yp}(z^{-1}) = \frac{A(z^{-1})S(z^{-1})}{P(z^{-1})} \ ; \qquad (6)$$

- Input sensitivity function (the transfer function between the disturbance $p(t)$ and the input of the system $u(t)$):

$$S_{up}(z^{-1}) = -\frac{A(z^{-1})R(z^{-1})}{P(z^{-1})} \ , \qquad (7)$$

where

$$P(z^{-1}) = A(z^{-1})S(z^{-1}) + z^{-d}B(z^{-1})R(z^{-1}) = A(z^{-1})S'(z^{-1}) \cdot H_S(z^{-1}) + z^{-d}B(z^{-1})R'(z^{-1}) \cdot H_R(z^{-1}) \qquad (8)$$

defines the poles of the closed loop (roots of $P(z^{-1})$).
In pole placement design, the polynomial $P(z^{-1})$ specifies the desired closed loop poles and the controller polynomials $R(z^{-1})$ and $S(z^{-1})$ are minimal degree solutions of (8) where the degrees of P, R and S are given by: $n_P \leq n_A + n_B + d - 1$, $n_S = n_B + d - 1$ and $n_R = n_A - 1$.
Using equations (2) and (3), one can write the output of the system as:

$$y(t) = \frac{A(q^{-1})S(q^{-1})}{P(q^{-1})} \cdot p(t) = S_{yp}(q^{-1}) \cdot p(t) \ . \qquad (9)$$

For more details on *RS*-type controllers and sensitivity functions see [21].

[3]The complex variable z^{-1} will be used for characterizing the system's behavior in the frequency domain and the delay operator q^{-1} will be used for describing the system's behavior in the time domain.

Suppose that $p(t)$ is a deterministic disturbance, so it can be written as

$$p(t) = \frac{N_p(q^{-1})}{D_p(q^{-1})} \cdot \delta(t) \ , \tag{10}$$

where $\delta(t)$ is a Dirac impulse and $N_p(z^{-1})$, $D_p(z^{-1})$ are coprime polynomials in z^{-1}, of degrees n_{N_p} and n_{D_p}, respectively. In the case of stationary disturbances the roots of $D_p(z^{-1})$ are on the unit circle (which will be the case for the disturbances considered in the benchmark). The energy of the disturbance is essentially represented by D_p. The contribution of the terms of N_p is weak compared to the effect of D_p, so one can neglect the effect of N_p. Figure 5 gives the frequency characteristics of the identified parametric models for the primary and secondary path (the excitation signal was a PRBS). The system itself in the absence of the disturbances will feature a number of low damped vibration modes as well as low damped complex zeros (anti-resonance). This will make the design of the controller difficult for rejecting disturbances close to the location of low damped complex zeros. The most significant are those near 50 Hz (secondary path) and 100 and 120 Hz (primary and secondary paths) (see the zoom of the frequency characteristics of the secondary path in figure 6). The range of frequencies for the disturbances considered in the benchmark is from 50 Hz to 95 Hz. Note that the design of a linear controller for rejecting a disturbance at 95 Hz is difficult since this frequency is close to a pair of very low damped zeros. The parametric models of both the secondary and primary path are of significant high order ($n_A = 23, n_B = 26$ and $n_C = 17, n_D = 16$ respectively). Data

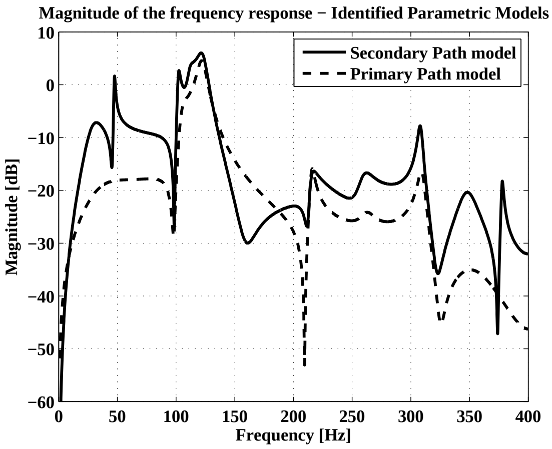

Fig. 5. Comparison between the magnitude of the frequency response for both models.

used for system identification are available on the website. The contributors had the possibility to use the models provided on the website or to identify models from the data provided (only Callafon *et al.* took this opportunity). They were also entitled to ask for a special experiment (nobody took this opportunity). The organizers provided an additional model for the secondary path obtained under different experimental conditions corresponding to a lower level of noise (by modifying the scaling of the A/D converter - however this does not correspond to the benchmark operating conditions). Figure 7 shows a

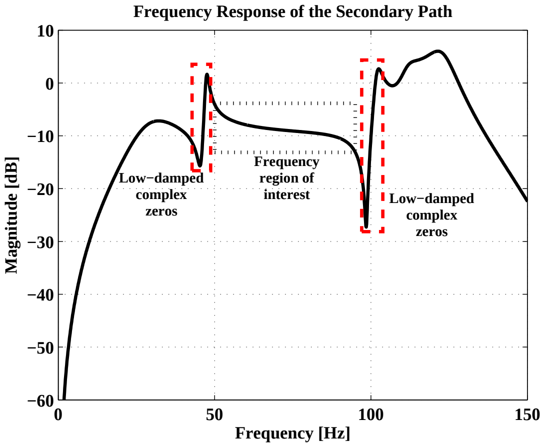

Fig. 6. Zoom at the magnitude of the secondary path's frequency response, between 0 and 150 Hz (website model).

comparison of the frequency characteristics of the two models. Some of the participants used this second model for tuning their controller for the real-time experiments(Aranovskiy *et al*, Callafon *et al.*).

It was assumed that all the contributors were familiar with the

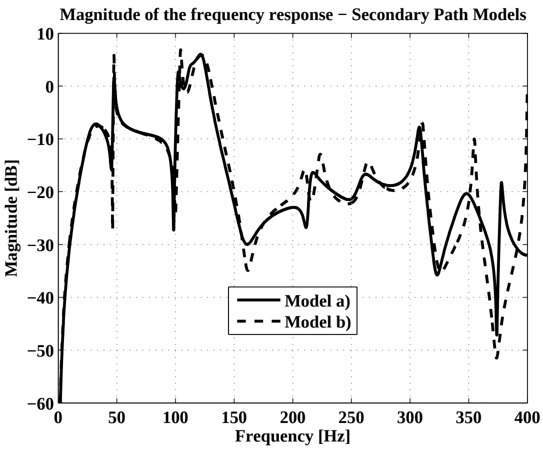

Fig. 7. Comparison between the magnitude of the frequency response for the identified models of the secondary path - a) website model, b) additional model.

design of linear controllers in the presence of very low damped complex zeros and the uncertainty generally associated with the value of the identified damping. No constraints have been imposed by the benchmark on the input sensitivity function. It turns out that all the contributors used the models provided by the organizers.

IV. Control specifications

The narrow band disturbances are located in the range 50 to 95 Hz. It is important to take into account the fact that the secondary path (the actuator path) has no gain at very low frequencies and very low gain in high frequencies near 0.5 F_s. Therefore the control system has to be designed such that the gain of the controller be very low (or zero) in these regions (preferably 0 at 0.5 F_s). Not taking into account these

constraints can lead to undesirable stress on the actuator.
There are three level of difficulty corresponding to one, two or three unknown time varying narrow band disturbances.

- **Level 1**: Rejection of a single time varying sinusoidal disturbance within 50 and 95 Hz.
- **Level 2**: Rejection of two time varying sinusoidal disturbances within 50 and 95 Hz.
- **Level 3**: Rejection of three time varying sinusoidal disturbances within 50 and 95 Hz.

The control objectives for all levels are summarized in Table I. Level 3 is particularly difficult in terms of tolerated amplification (at other frequencies than those of the disturbances) and transient requirements.
In order to test the required performances, 3 protocols have been defined:
Protocol 1. Tuning capabilities: Evaluation in steady state operation after application of the disturbance once the adaptation settles. *This is the most important aspect of the benchmark.*
Test 1: The steady state performance in time domain will be evaluated by measuring the mean square value of the residual force which will be compared with the value of the residual force in open loop (providing a measure of the global attenuation).
Test 2: Power spectral density performances. For constant frequency disturbances, once the adaptation transient is settled, the performance with respect to the open loop will be evaluated as follows:

- Attenuation of the disturbances (with respect to the open loop) should be larger than the specified value.
- Amplification at other frequencies (with respect to the open loop) should be less than the specified value.

Protocol 2. Transient performance in the presence of step application of the disturbance and step changes in the frequency of the disturbances.
Test 1: Step application of the disturbances.
Test 2: Step changes in the frequencies of the disturbances. The frequencies of the disturbances around specified central values are changed by $+/-5$ Hz. An upper bound for the duration of the adaptation transient was imposed (2 sec). However it was not possible to define a reliable test for measuring the duration of the transient. The quantities which have been measured for the purpose of performance evaluation are:

- the square of the truncated two-norm of the residual force over a time horizon;
- the maximum value of the residual force during transient.

Protocol 3. Chirp changes in frequency.
Linear time varying frequency changes between two situations are considered. The maximum value of the residual force during the chirp has been measured as well as the mean square value of the residual force.
The loop is closed before the disturbances are applied for all the above tests.

Supplementary tests:

- The operation of the system should remain stable for all the levels if one, two or three sinusoidal disturbances are applied simultaneously.
- The operation of the loop should remain stable if the disturbance is applied simultaneously with the closing of the loop.

TABLE I
CONTROL SPECIFICATIONS IN THE FREQUENCY DOMAIN.

Control specifications	Level 1	Level 2	Level 3
Transient duration	$\leq$ 2 sec	$\leq$ 2 sec	$\leq$ 2 sec
Global attenuation	$\geq$ 30 dB*	$\geq$ 30 dB	$\geq$ 30 dB
Minimum disturbance attenuation	$\geq$ 40 dB	$\geq$ 40 dB	$\geq$ 40 dB
Maximum amplification	$\leq$ 6 dB	$\leq$ 7 dB	$\leq$ 9 dB
Chirp speed	10 Hz/sec	6.25 Hz/sec	3 Hz/sec
Maximum value during chirp	$\leq$ 0.1 V	$\leq$ 0.1 V	$\leq$ 0.1 V

* For this level, the specification of 30 dB is for the range between 50 and 85 Hz, for 90 Hz is 28 dB and for 95 Hz is 24 dB.

Routines for executing the protocols and the measurements have been provided (see website).
The complexity of the procedures proposed have been evaluated by measuring the average *Task Execution Time* on the real-time system.

Additional tests in simulation and real time have been done by the organizers in order to test the tuning capabilities and transient performance within the range of frequencies considered in the benchmark but with different experimental protocols (testing others values for the frequencies within the given range, changing the spacing between the narrow band disturbances in the case of level 2 and 3, changing the time of application of the disturbances).

Global criteria have been used to asses the performance of each procedure and to allow a comparison between the various schemes (See section VIII).

V. COHERENCE OF SIMULATION RESULTS AND EXPERIMENTAL RESULTS

There were some differences between the real plant and the simulator. They can be summarized as follows:

- A small bias in the force measurement is present on the real system (easy to compensate).
- The noise in the simulator was a sample of the noise measured on the real system in the absence of signals. Some differences occur in the presence of disturbance and compensation. This can be explained by the presence of some harmonics of the disturbances (a low level) since neither the disturbance generator nor the inertial actuator are perfectly linear.
- Uncertainties in the estimation of the frequency and damping of the very low damped complex zeros (see figure 7) located near 50 Hz and 95 Hz.
- Some uncertainties on the model in the frequency region over 150 Hz (see figure 7).

Some of the contributors got in the first experiments significant differences between simulation results and real-time results. These differences can be classified in two categories:

1) instabilities in some situations,
2) significant differences in performance in other situations.

In fact these problems have been easily solved by imposing on *tuned* controllers a very low level of the input sensitivity function around the low damped complex zeros located close to the border of the operation region and outside the operation region (which implies very good robustness with respect to additive uncertainties).

One can conclude that the basic rule is to have gain in the controller only in the frequency region of operation (50 to 95 Hz) and very low gain outside.

VI. Methodological Comparison

Before going to evaluate the performance of the various approaches, it is important to asses from a methodological point of view what are the resemblances and the differences between the various approaches proposed. Most of the proposed approaches use implicitly or explicitly a *Youla-Kučera* parametrization of the controller. This also leads to the presence of an observer for the (non measurable) disturbance, which uses the measurements of the input and the output of the system (see figure 8).

However, the *Youla-Kučera* parametrization is not unique, it depends of the right coprime factorization selected $G = ND^{-1}$. For the benchmark problem where the plant is

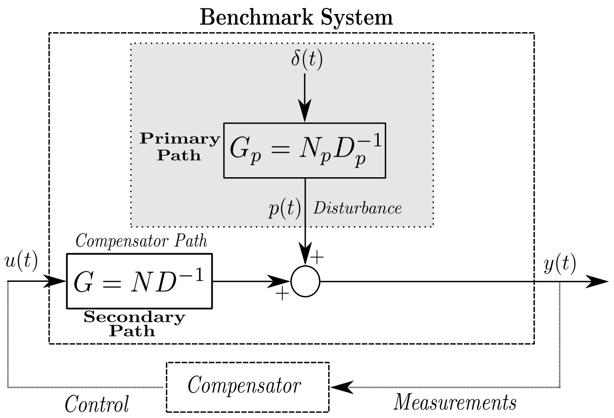

Fig. 8. General Scheme for the benchmark system.

SISO, four factorizations have been considered by the various contributors:

Factorization 1

$$N = G; \quad D = I. \tag{11}$$

This factorization leads to an *output error* disturbance observer (see figure 9) with

$$w_{OE} = y - Gu. \tag{12}$$

Factorization 2

$$N = z^{-m}; \quad D = P_m \quad \text{with} \quad G \approx z^{-m} P_m. \tag{13}$$

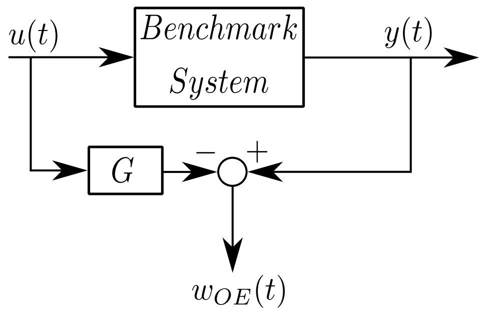

Fig. 9. Output Error factorization scheme.

This factorization leads in fact to an *input error* observer (see figure 10) with

$$w_{iu} = q^{-m} u - P_m^{-1} y. \tag{14}$$

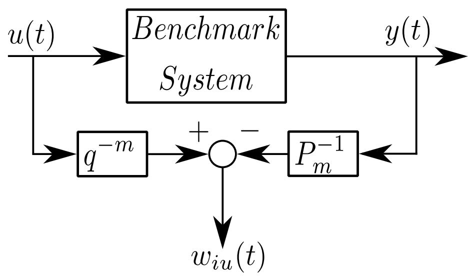

Fig. 10. Input Error factorization scheme.

Factorization 3

$$N = B; \quad D = A \quad \text{with} \quad G = B/A. \tag{15}$$

This factorization leads to an *equation error* disturbance observer (see figure 11) with

$$w_{EE} = Ay - Bu. \tag{16}$$

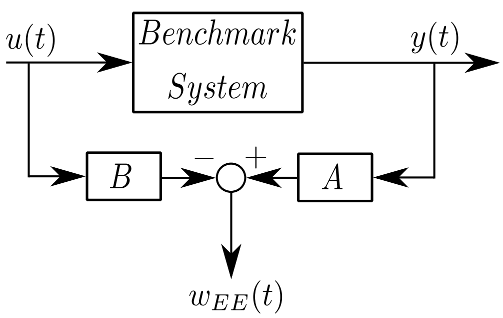

Fig. 11. Equation Error factorization scheme.

Factorization 4

$$N = BF; \quad D = AF \quad \text{with} \quad G = B/A; \quad F = F_N/F_D. \tag{17}$$

with F and F^{-1} asymptotically stable. This factorization leads to a *filtered equation error* disturbance observer (see figure 12) with

$$w_{FEE} = AFy - BFu = Fw_{EE}. \tag{18}$$

The filtered equation error disturbance error can be obtained either by using the filtered factors or using the equation error disturbance observer and filtering this quantity by F(see figure 12 a and b respecitvely) . Implicitly those configurations which use the equation error disturbance observer but include a fixed filter in cascade with the Q filter correspond in fact to a filtered equation error observer configuration.

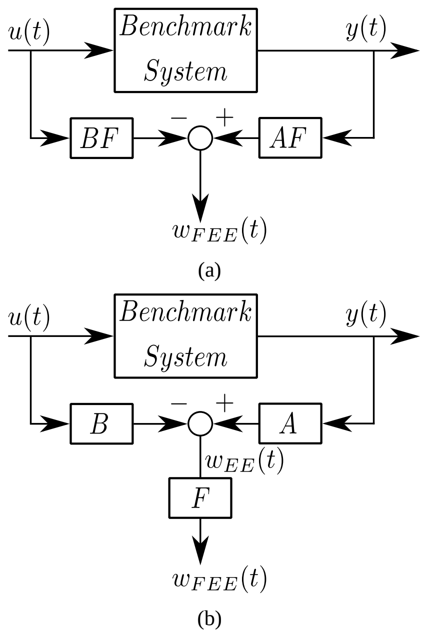

Fig. 12. Filtered Equation Error Factorization - Two equivalent schemes.

Table II tries to emphasize the characteristics of each proposed approach for the benchmark. The presence (or absence) of the *central controller* (controller used in the absence of disturbance) is indicated as well the design method used for the central controller. The list of acronyms used is given below.

List of acronyms for Table II.

IMP	-	Internal model principle
TF	-	Transfer function
FIR	-	Finite impulse response
IIR	-	Infinite impulse response
LQR	-	Linear quadratic regulator
LPV	-	Linear parameter varying control
n	-	Number of narrow band (sinusoidal) disturbances
a.s.	-	Asymptotically stable

Callafon *et al.* and Wu *et al.* provided a single controller configuration valid for all the three levels. Aranovskiy *et al* provided both a single controller configuration valid for all three levels as well specific configurations for each level. It was found that in real time the specific configurations gave better performance that the single configuration and therefore the results are given for case of specific configuration for each level. Airimitoaie *et al* provided a single central controller but the frequency estimator was different for each level. The other contributors provided a specific controller configuration for each level (in terms of central controller and parameter estimator).

All participants except Aranovskiy *et al.* and Callafon *et al.* provided the same controller for simulations and real-time experiments. Aranovskiy *et al.* have used the model of the secondary path given on the website for the implementation of the controllers used in simulation and the additional model of the secondary path (see figure 7) for the implementation of the controllers used in real time.

VII. Measurements for Performance Analysis

In order to assess the performance of the proposed approaches, measurement procedures have been defined. These measurements will give information both for *steady state* and *transient* behavior.

A. Measurements for Simple Step test

For step application of the disturbance, measurements for the transient behavior and steady state behavior (tuning capabilities) have been defined. The benchmark protocol for the *Simple Step* test defines the time period for the disturbance application. The disturbance is applied at $t = 15$ seconds, while the entire experiment duration is 30 seconds. In this context, the *transient* behavior will be considered in the first 3 seconds after the disturbance is applied. For measuring the *steady state* behavior the last 3 seconds of the test (before the disturbance is removed), will be used since it is expected that the algorithm has converged at this time.

The measurements considered in time domain are:

- The *square of the truncated two norm* of the residual force defined by
$$N^2T = \sum_{i=1}^{m} y(i)^2,$$
where $y(i)$ is a sample of the discrete-time signal to evaluate. This quantity indicates the *energy* contained in the measured signal.
- The *maximum value* measured in millivolts and defined by
$$MV = \max_{m} |y(i)|.$$

The measurements in frequency domain (steady state behaviour) are:

- *Global Attenuation* (GA) measured in dB and defined by
$$GA = 20\log_{10}\frac{N^2Y_{ol}}{N^2Y_{cl}},$$
where Y_{ol} and Y_{cl} correspond to the last 3 seconds of the measured residual force in open and closed loop, respectively.
- *Disturbance Attenuation* (DA) measured in dB and defined as the minimum value of the difference between the estimate PSD[4] of the residual force in closed loop and in open loop:
$$DA = \min\left(\text{PSD}_{cl} - \text{PSD}_{ol}\right).$$
- *Maximum Amplification* (MA) measured in dB, is defined as the maximum value of the difference between the

[4]Power Spectral Density.

TABLE II

COMPARATIVE TABLE FOR THE DIFFERENT APPROACHES USED IN THE BENCHMARK

Participant	Plant Factorization $G = ND^{-1}$	Disturbance Observer For Control	YK Parame-trization	Type of Q Filter	Central Controller Design	Disturbance Rejection Method	Type of Adaptation	Number of Parameters to Adapt	Error Signal For Adaptation
Aranovskiy *et al.*	$N = L$ $D = I$ $L = G$ or *a.s. T.F.*	Output error	Yes	FIR filter cascaded with fixed filter or Bench of weighted parallel filters (IIR/FIR)	No central controller (can be added)	IMP	Direct	$2n$	Disturbance estimation (OE)
Callafon *et al.*	$N = BF$ $D = AF$ $F = F_N/F_D$ or 1 $F, F^{-1} = a.s.$	Equation error	Yes	FIR	H_2	H_2	Direct	Any. Benchmark: $n = 29$	Performance Indicator *vector* (crit. arg)
Karimi *et al.*	$N = B$ $D = A$	No	No	No	No	H_∞+IMP	Indirect (LPV with interpol.) Gain Sche.	n	Disturbance Estimation (OE)
Wu *et al.*	$N = B$ $D = A$	Equation error	Yes	FIR filter cascaded with fixed BP filter	LQR	IMP	Direct	$2n$	Residual error estimation
Xu *et al.*	$N = z^{-m}$ $D = P_m^{-1}$ $G \approx z^{-m}P_m$	Input error	Yes	IIR (notch filter structure)	Stability	Plant Model Approx. Inversion (IMP)	Direct	n	Disturbance estimation (OE)
Airimitoaie *et al.*	$N = B$ $D = A$	Equation error	Yes	IIR filter cascaded with fixed filter	Pole Placement	Output sensitivity shaping	Indirect	n	Disturbance Estimation (OE)
Castellanos *et al.*	$N = B$ $D = A$	Equation error	Yes	FIR filter cascaded with fixed filter	Pole placement	IMP	Direct	$2n$	Residual error estimation

estimate PSD of the residual force in closed and open loop:

$$MA = \max\left(\text{PSD}_{cl} - \text{PSD}_{ol}\right).$$

For all the frequency domain measurements, only the last 3 seconds of the test are considered.

B. Measurements for Step Frequency Changes

For the *Step Frequencies Changes* only time domain measurements were considered. Based on the protocol for this test, a frequency step change occurs every 3 seconds. During this time period the following measurements are considered:

- Square of the truncated two norm of the transient N^2T.
- Maximum value of the transient MV.

C. Chirp Frequency Change

For the *Chirp* Test only time domain measurements were considered. The measurements are:

- Mean Square of the residual force defined as

$$MSE = \frac{1}{m}\sum_{i=1}^{m} y(i)^2 = \frac{1}{m}N^2T,$$

  where m correspond to the number of output samples evaluated.
- Maximum value MV measured in millivolts.

VIII. EVALUATION CRITERIA

The results of each group will be evaluated with respect to the benchmark specifications. However, for some performance indices no bounds have been set in the benchmark and the comparison will be done between the various indices obtained. To summarize, two types of criteria will be considered:

- criteria for taking in account the fact that not all the specifications have been satisfied (when applicable),
- normalized quantitative criteria for comparison of performance indices for which benchmark specifications were not available.

Evaluation of the performances will be done for both simulation and real-time results. The simulation results will give us information upon the potential of the design methods under the assumption: *design model* = *true plant model*. The real-time results will tell us in addition what is the robustness of the design with respect to plant model uncertainties and real noise. These criteria are given next.

A. Steady State Performance (Tuning capabilities)

As mentioned earlier, these are the most important performances. Only if a good tuning with respect to disturbance can be obtained, it makes sense to examine the transient performance of a given scheme. For the steady state performance, which is evaluated only in the *simple step test*, the variable k, with $k = 1, \ldots, 3$, will indicate the *level* of the benchmark. In several criteria a mean of certain variables will be considered. The number of measurements, M, is used to compute the mean. This number depend upon the level of the benchmark as follows:

$$\begin{aligned} M &= 10, \quad \text{if} \quad k=1 \\ M &= 6, \quad \text{if} \quad k=2 \\ M &= 4, \quad \text{if} \quad k=3 \end{aligned}$$

The performances can be evaluated with respect to the benchmark specifications. The benchmark specifications will be in the form: XXB, where XX will denote the evaluated variable and B will indicate the benchmark specification. ΔXX will represent the error with respect to the benchmark specification.

1) Global Attenuation - GA: The benchmark specification corresponds to $GAB_k = 30$ dB, for all the levels and frequencies, except for 90 Hz and 95 Hz at $k=1$, for which GAB_1 is 28 dB and 24 dB respectively.

Error:

$$\begin{aligned} \Delta GA_i &= GAB_k - GA_i \quad \text{if} \quad GA_i < GAB_k \\ \Delta GA_i &= 0 \quad \text{if} \quad GA_i \geq GAB_k \end{aligned}$$

with $i = 1, \ldots, M$.

Global Attenuation Criterion

$$J_{\Delta GA_k} = \frac{1}{M} \sum_{j=1}^{M} \Delta GA_i \tag{19}$$

2) Disturbance Attenuation - DA: The benchmark specification corresponds to $DAB = 40$ dB, for all the levels and frequencies.

Error:

$$\begin{aligned} \Delta DA_{ij} &= DAB - DA_{ij} \quad \text{if} \quad DA_{ij} < DAB \\ \Delta DA_{ij} &= 0 \quad \text{if} \quad DA_{ij} \geq DAB \end{aligned}$$

with $i = 1, \ldots, M$ and $j = 1, \ldots, j_{max}$, where $j_{max} = k$.

Disturbance Attenuation Criterion

$$J_{\Delta DA_k} = \frac{1}{M} \sum_{i=1}^{M} \sum_{j=1}^{j_{max}} \Delta DA_{ij} \tag{20}$$

3) Maximum Amplification - MA: The benchmark specifications depend on the level, and are defined as

$$\begin{aligned} MAB_k &= 6, \quad \text{if} \quad k=1 \\ MAB_k &= 7, \quad \text{if} \quad k=2 \\ MAB_k &= 9, \quad \text{if} \quad k=3 \end{aligned}$$

Error:

$$\begin{aligned} \Delta MA_i &= MA_i - MAB_k, \quad \text{if} \quad MA_i > MAB_k \\ \Delta MA_i &= 0, \quad \text{if} \quad MA_i \leq MAB_k \end{aligned}$$

with $i = 1, \ldots, M$.

Maximum Amplification Criterion

$$J_{\Delta MA_k} = \frac{1}{M} \sum_{i=1}^{M} \Delta MA_i \tag{21}$$

4) Global criterion of steady state performance for one level:

$$J_{SS_k} = \frac{1}{3}[J_{\Delta GA_k} + J_{\Delta DA_k} + J_{\Delta MA_k}] \tag{22}$$

5) Benchmark Satisfaction Index for Steady State Performance: Following the procedure for the *robust digital control benchmark* [16] a *Benchmark Satisfaction Index* can be defined.

The *Benchmark Satisfaction Index* is a performance index computed from the *average* criteria $J_{\Delta GA_k}$, $J_{\Delta DA_k}$ and $J_{\Delta MA_k}$. The *Benchmark Satisfaction Index* is 100%, if these quantities are "0" (full satisfaction of the benchmark specifications) and it is 0% if the corresponding quantities are half of the specifications for *GA*, and *DA* or twice the specifications for *MA*. The corresponding reference error quantities are summarized below:

$$\begin{aligned} \Delta GA_{index} &= 15, \\ \Delta DA_{index} &= 20, \\ \Delta MA_{index,1} &= 6, \quad \text{if} \quad k=1, \\ \Delta MA_{index,2} &= 7, \quad \text{if} \quad k=2, \\ \Delta MA_{index,3} &= 9, \quad \text{if} \quad k=3. \end{aligned}$$

The computation formulas are

$$\begin{aligned} GA_{index,k} &= \left(\frac{\Delta GA_{index} - J_{\Delta GA_k}}{\Delta GA_{index}} \right) 100\% \\ DA_{index,k} &= \left(\frac{\Delta DA_{index} - J_{\Delta DA_k}}{\Delta DA_{index}} \right) 100\% \\ MA_{index,k} &= \left(\frac{\Delta MA_{index,k} - J_{\Delta MA_k}}{\Delta MA_{index,k}} \right) 100\%. \end{aligned}$$

Then the *Benchmark Satisfaction Index* (BSI), is defined as

$$BSI_k = \frac{GA_{index,k} + DA_{index,k} + MA_{index,k}}{3} \tag{23}$$

The results for BSI_k obtained both in simulation and real-time for each participant and all the levels are summarized in Table III, and represented graphically in figure 13. Table III shows also the J_{SS_k} for all the levels and contributors. Low values of J_{SS_k} indicate an "average" good performance. However Benchmark Satisfaction Index (BSI_k) allows a better characterization of the performance with respect to the various benchmark specifications. The results obtained in simulation allows to characterize the performance of the proposed design under the assumption that *design model = true plant model*. Therefore in terms of capabilities of a design method to meet the benchmark specification the simulation results are fully relevant. It is also important to recall that Level 3 of the benchmark is the most important. The results obtained in real time, more exactly the difference between the simulation results and real time results, allow to characterize the robustness in performance with respect to uncertainties on design model and noise model (for those who used the same controller in simulation and in real time).

TABLE III
BENCHMARK SATISFACTION INDEX FOR ALL THE PARTICIPANTS

Participant	LEVEL 1				LEVEL 2				LEVEL 3			
	Simulation		**Real Time**		**Simulation**		**Real Time**		**Simulation**		**Real Time**	
	J_{SS_1}	BSI_1	J_{SS_1}	BSI_1	J_{SS_2}	BSI_2	J_{SS_2}	BSI_2	J_{SS_3}	BSI_3	J_{SS_3}	BSI_3
Aranovskiy *et. al.*	0.87	86.94%	1.20	80.22%	1.77	76.33%	2.04	73.58%	0.84	90.65%	1.41	84.89%
Callafon *et. al.*	2.12	89.21%	6.74	49.37%	5.02	72.89%	11.01	29.08%	17.14	51.74%	31.47	8.40%
Karimi *et. al.*	1.33	91.92%	2.17	72.89%	3.42	76.13%	7.43	44.33%	-	-	-	-
Wu *et. al.*	0.11	98.31%	1.31	**83.83%**	0.13	98.48%	1.35	84.69%	0.18	98.01%	1.34	91.00%
Xu *et. al.*	**0.00**	**100.00%**	**1.00**	**86.63%**	**0.00**	**100.00%**	1.37	**86.65%**	**0.04**	**99.78%**	1.45	92.52%
Airimitoaie *et. al.*	0.08	98.69%	1.23	81.11%	0.11	98.38%	**0.94**	**88.51%**	0.11	99.44%	1.58	90.64%
Castellanos *et. al.*	0.50	93.30%	1.35	80.87%	0.29	97.29%	1.20	**89.56%**	0.17	99.13%	**0.43**	**97.56%**

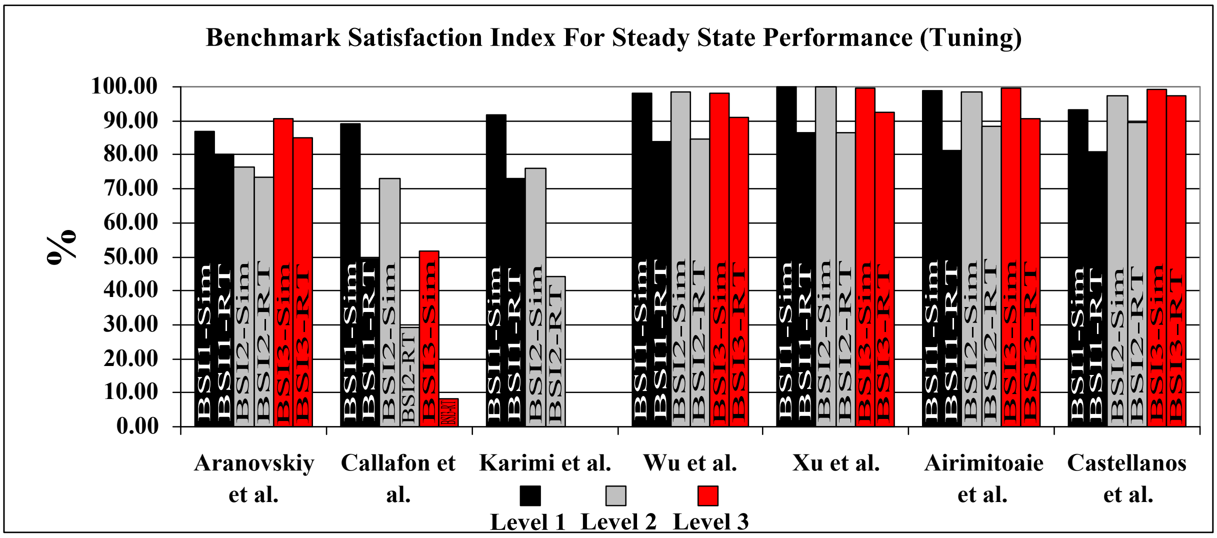

Fig. 13. Benchmark Satisfaction Index (*BSI*) for all levels and all participants, both in simulation and real-time.

B. Simulation Results

Consider the *simulation results* in terms of the BSI. Clearly the *benchmark specifications* are achievable since Xu *et. al.* have achieved 100% for Level 1 and 2 and for Level 3 Xu et al. and Airimitoaie *et. al.* have achieved respectively 99.78% and 99.44%. If we look for those who achieved at least 97% of the benchmark specifications, for Level 1 one find Xu *et. al.*, Airimitoaie *et. al.* and Wu *et. al.* For Level 2 and 3, one find Xu *et. al.*, Airimitoaie *et. al.* and Wu *et. al.* and Castellanos *et. al.* These designs feature a number of common properties as well as some differences.

- They all use a Youla Kučera parametrization.
- Xu *et al.*, and Wu *et al.* and Castellanos *et al.* use the IMP and direct adaptation.
- Airimitoaie *et al.* uses shaping of the output sensitivity function and indirect adaptation.

The approach of Callafon *et al.* has been probably handicapped by the fact that the real-time control system did not allow to use more than 29 adjustable parameters and this number has been used also in simulations. One has also to mention that Karimi *et al.*, which use a convex optimization procedure, were not able to provide controllers for the Level 3.

C. Real Time Results

Rigourously the same algorithms and tunings from simulation have been used for the real time experiments by all the participants except Aranovskiy *et al.*and Callafon *et al.* (which use different models for building the controllers for simulation and real time experiments).
The physical system can not be considered as a ”deterministic system” in particular concerning the noise (but not only). Therefore a very precise evaluation of the performance would require that an average of several repetitive tests (let say 10) be considered as the relevant information. Unfortunately this was not possible to be done taking in account the large number of trials to be done. However for one situation (Level 3) and for one controller configuration but considering two protocols, multiple experiments have been conducted and the results have been analyzed. The conclusion is that the results which are provided for the BSI in Table III have to be considered with an associate uncertainty of about $+/-4\%$. The consequence is that we can not classify results within this uncertainty range.

From Table III it result that for Level 1 the best results have been obtained by Xu *et. al.* and Wu *et al.*. For Level 2 the best results have been obtained by Castellanos *et al.*, Airimitoaie et al. and Xu *et al.*. For Level 3 the best results have been obtained by Castellanos *et al.*[5].

Since there are differences between simulation results and real time results it is interesting to asses the robustness with respect to model uncertainties.

[5] All these mentioned results differ by less than 4% with respect to the highest value obtained

D. Robustness with respect to model uncertainties

As it was mentioned earlier there are uncertainties on the plant model used for design. These uncertainties come mostly from the difficulty of correctly identifying very low damped complex zeros. The identification results concerning the low damped complex zeros are influenced by the level of noise. As mentioned earlier (see Section V) also the noise is different in the simulator with respect to the real system. The contributors were aware of these problems and the final designs did not show any instability going from the simulation scheme to the real system.
However the loss in performance moving from simulation to real time experiments is obvious as it can be seen in Table III. Therefore an important point is to asses the robustness in performance for those which use the same controller in simulation and in real time. This will be done by defining the *Normalized Performance Loss*.

For each level one defines the *Normalized Performance Loss* as:

$$NPL_k = \left(\frac{BSI_{ksim} - BSI_{kRT}}{BSI_{ksim}}\right) 100\% \tag{24}$$

and the global NPL is given by

$$NPL = \frac{1}{M}\sum_{k=1}^{M} NPL_k \tag{25}$$

where $N = 3$ for all the participants except for Karimi *et al.*, since they provided only solutions for levels 1 and 2; for them $N = 2$.

Table IV gives the normalized performance loss for all the participants and levels. The figure 14 summarizes in a bar graph these results. The results for Aranovskiy *et al.* and Callafon *et al.* are given for information only since the controllers are not the same in simulation and real time.

TABLE IV
NORMALIZED PERFORMANCE LOSS FOR ALL THE PARTICIPANTS

Participant	NPL_1	NPL_2	NLP_3	NPL
Aranovskiy *et al.*	7.73%*	3.61%*	6.35%*	5.90%*
Callafon *et al.*	44.66%	60.11%	83.77%	62.85%
Karimi *et al.*	20.70%	41.77%	-	31.24%
Wu *et al.*	14.73%	14.01%	7.16%	11.96%
Xu *et al.*	13.37%	13.35%	7.28%	11.33%
Airimitoaie *et al.*	17.81%	10.03%	8.85%	12.23%
Castellanos *et al.*	**13.32%**	**7.95%**	**1.58%**	**7.62%**

For the Levels1, 2 and 3, the design of Castellanos *et al.* has the minimum $NPL_{2,3}$. The minimum averaged NPL has been obtained by Castellanos *et al.* For Callafon *et al.* the explanation of a high loss in performance come from the fact that the controller gain in high frequencies (over 100 Hz) has not been reduced enough.

E. Transient Performance

Transient performances will be evaluated for

- Simple Step Test (application of the disturbance).
- Step Changes in the frequencies.
- Chirp Changes in the frequencies.

We will consider first the case of the *simple step test*.

1) Simple Step Test: The basic specification for transient performance is the requirement that the transient duration when a disturbance is applied, be smaller than 2 sec. Similar to the steady state performance a BSI index for transient duration has been established (a transient duration of 4 sec corresponds to 0%). From the point of view of the benchmark, this means that 2 sec. after application of a disturbance the square of the truncated two norm has to be equal or smaller than 1.21 of the steady state value of the square of the truncated two norm of the residual force. The square of the truncated two norm is evaluated over an interval of 3 sec both for transient and steady state, taking in account that disturbance is applied at t=5 sec and that steady state is evaluated between 17 and 20 sec. The square of the truncated two norm is denoted as $N2T(v:w)$ where v and w define the interval of computation. One define:

$$\begin{aligned}
\alpha_i &= \frac{N2T(7:10)}{N2T(17:20)} \\
\Delta Trans_i &= \alpha_i - 1.21 \quad \text{if} \quad \alpha_i > 1.21 \\
\Delta Trans_i &= 0 \quad \text{if} \quad \alpha_i \leq 1.21 \\
i &= 1,\dots,M
\end{aligned}$$

$$J_{\Delta Trans_k} = \frac{1}{M}\sum_{j=1}^{M} \Delta Trans_i \tag{26}$$

$$\begin{aligned}
BSI_{Trans_k} &= \left(\frac{1.21 - J_{\Delta Trans_k}}{1.21}\right) 100\% \\
k &= 1,\dots,3
\end{aligned} \tag{27}$$

where M is given by

$$\begin{aligned}
M &= 10, \quad \text{if} \quad k = 1 \\
M &= 6, \quad \text{if} \quad k = 2 \\
M &= 4, \quad \text{if} \quad k = 3
\end{aligned}$$

Table V gives the results obtained for the various approaches. Most of the approaches have met the specifications or are very close.
The transient performances have been further investigated in order to compare the various approaches. Simple step test, step changes in frequencies and chirp tests have been considered. Two quantities have been defined.

- Square of the truncated-two norm of residual force N^2T.
- Maximum value during transient MV.

Note: In order to introduce "normalized" criteria (maximum value $= 1$) one has to define for these 2 quantities the $(Max)_{\max}$ within the results provided by all the participants. These quantities will be called $(J^U_{NT_k})_{\max}$, $(J^U_{MV_k})_{\max}$, where the U stands for *un-normalized*.

$$\begin{aligned}
J^U_{NT_k} &= \frac{1}{M}\sum_{i=1}^{M} N^2T(i) \\
J^U_{MV_k} &= \frac{1}{M}\sum_{i=1}^{M} MV(i)
\end{aligned}$$

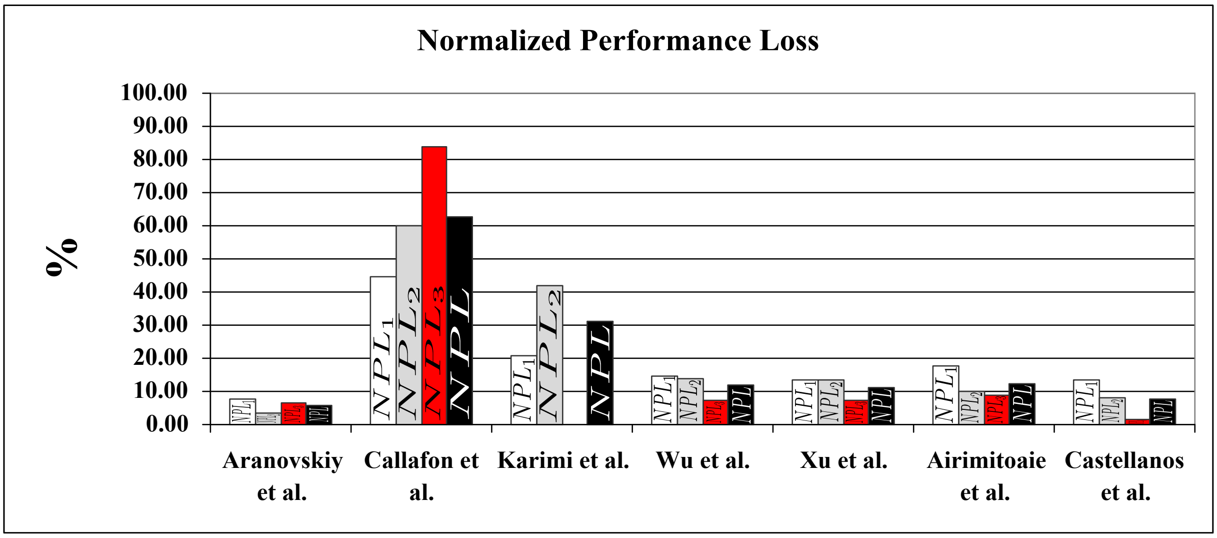

Fig. 14. Normalized Performance Loss (*NPL*) for all levels and all participants.

TABLE V
BENCHMARK SATISFACTION INDEX FOR TRANSIENT PERFORMANCE(FOR SIMPLE STEP TEST)

Participant \ Index	$\mathbf{BSI_{Trans_1}}$		$\mathbf{BSI_{Trans_2}}$		$\mathbf{BSI_{Trans_3}}$	
	Simulation	Real Time	simulation	Real Time	Simulation	Real Time
Aranovsikiy *et al.*	100%	100%	100%	100%	100%	100%
Callafon *et al.*	100%	100%	100%	100%	100%	81.48%
Karimi *et al.*	100%	85.74%	100%	91.79%	-	-
Wu *et al.*	100%	99.86%	94.85%	100%	100%	92.40%
Xu *et al.*	100%	100%	100%	100%	100%	100%
Airimitoaie *et al.*	100%	99.17%	83.33%	100%	100%	100%
Castellanos *et al.*	100%	96.45%	100%	95.74%	100%	100%

TABLE VI
AVERAGE GLOBAL CRITERION FOR TRANSIENT PERFORMANCE FOR ALL THE PARTICIPANTS

Participant	**JTRAV1**		**JTRAV2**		**JTRAV3**	
	Simulation	**Real Time**	**Simulation**	**Real Time**	**Simulation**	**Real Time**
Aranovskiy *et al.*	0.76	0.89	0.57	0.72	0.51	0.61
Callafon *et al.*	0.44	0.54	**0.26**	**0.40**	**0.22**	0.52
Karimi *et al.*	**0.35**	**0.40**	0.34	0.49	-	-
Wu *et al.*	0.50	0.56	0.36	0.46	0.34	**0.37**
Xu *et al.*	0.39	0.55	0.76	0.81	0.63	0.74
Airimitoaie *et al.*	0.93	0.85	0.60	0.71	0.42	0.49
Castellanos *et al.*	0.55	0.61	0.48	0.60	0.90	0.98

$$J_{NT_k} = \frac{J^U_{NT_k}}{(J^U_{NT_k})_{\max}}$$

$$J_{MV_k} = \frac{J^U_{MV_k}}{(J^U_{MV_k})_{\max}}$$

where M is given by

$$M = 10, \quad \text{if} \quad k = 1$$
$$M = 6, \quad \text{if} \quad k = 2$$
$$M = 4, \quad \text{if} \quad k = 3$$

Global criterion for transient evaluation for simple step test:

$$J_{TR_k} = \frac{1}{2}\left[J_{NT_k} + J_{MV_k}\right] \tag{28}$$

2) Step Frequency Changes Test: Only the square of the norm of the residual force and the maximum value during transient will be considered (similar case to the simple step test). The corresponding criteria are given below.

$$J^U_{SNT_k} = \frac{1}{M}\sum_{i=1}^{M} N^2 T_i$$

$$J^U_{SMV_k} = \frac{1}{M}\sum_{i=1}^{M} MV_i$$

$$J_{SNT_k} = \frac{J^U_{SNT_k}}{(J^U_{SNT_k})_{\max}}$$

$$J_{SMV_k} = \frac{J^U_{SMV_k}}{(J^U_{SMV_k})_{\max}}$$

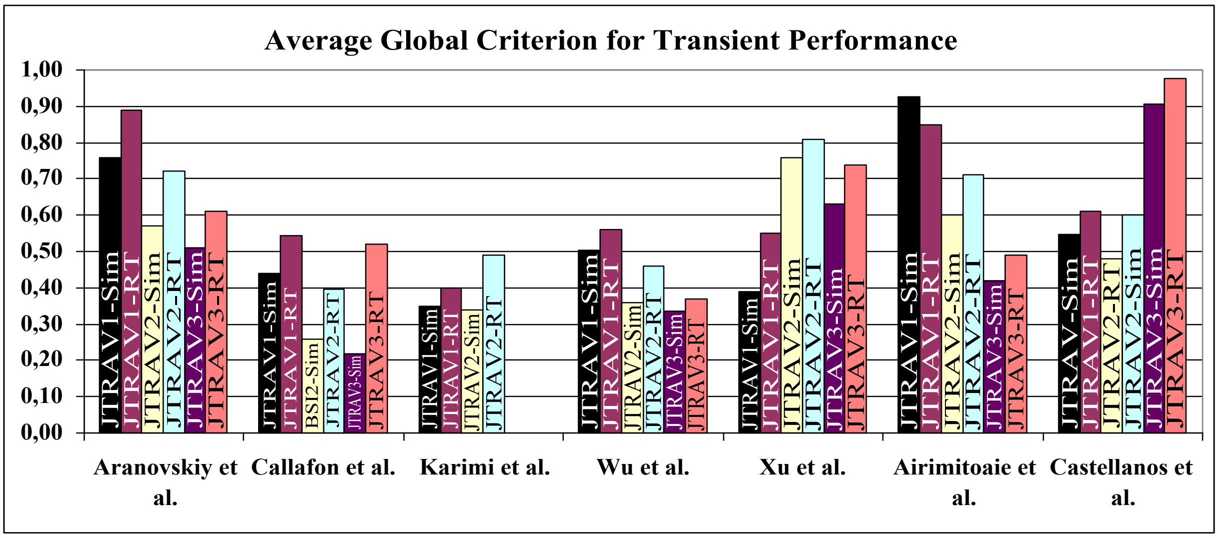

Fig. 15. Average global criterion for transient performance (J_{TRAV})for all levels and all participants.

where M is given by

$$M = 12, \quad \text{if} \quad k = 1$$
$$M = 8, \quad \text{if} \quad k = 2$$
$$M = 8, \quad \text{if} \quad k = 3$$

Global criterion for transient performance evaluation - step changes in frequencies:

$$J_{STR_k} = \frac{1}{2}\left[J_{SNT_k} + J_{SMV_k}\right] \tag{29}$$

3) Chirp Test: As for the Step Frequencies Changes , the maximum values among all the participants will be used to normalize the results. For each level two measurements have been done for:

- Mean Square of the residual force (MSE),
- Maximum Value of the residual force (MV),

during the periods of application of the chirp. They are denoted by *up* when the frequencies increase and *down* when the frequencies decrease.
One defines the criterion for the mean square error (for each level) for all the levels ($k = 1, \ldots, 3$) as follows[6]

$$J^U_{MSE_k} = \frac{1}{2}\left[MSE_{up} + MSE_{down}\right]$$
$$J_{MSE_k} = \frac{J^U_{MSE_k}}{(J^U_{MSE_k})_{\max}}$$

The benchmark specifications for the *maximum value* were far too conservative. However, a comparison between the various approaches has to be done.

For the maximum value one defines the criterion

$$J^U_{MV_k} = \frac{1}{2}\left[MV_{up} + MV_{down}\right]$$
$$J_{MV_k} = \frac{J^U_{MV_k}}{(J^U_{MV_k})_{\max}}$$

[6]the results are exactly the same for the normalized values J_{MSE_k} if one uses N^2T instead of MSE.

Global criterion for chirp disturbance:

$$J_{chirp_k} = \frac{1}{2}\left[J_{MSE_k} + J_{MV_k}\right] \tag{30}$$

An average global criterion for transient performance is defined for each level as:

4) ***Average Global criterion for transient performance (one level)****:*

$$J_{TRAV_k} = \frac{1}{3}[J_{TR_k} + J_{STR_k} + J_{chirp_k}] \tag{31}$$

Table VI gives the values of J_{TRAV_k} for all levels and participants, both in simulation and real-time. For this criterion lower values means a better transient behaviour. A graphic representation of these results is given in figure 15. Best results in simulation are obtained by Karimi *et al.* (Level 1), Callafon *et al.* (Levels 2 and 3). In real time the best results are obtained by Karimi *et al.* (Level 1), Callafon *et al.* (Levels 2) and Wu *et al.* (Level 3). The results of Karimi *et al.* can be explained by the fact that it is an interpolation between a set of stored controller and the parameters for interpolation are rapidly identified for Level 1 and 2 as well as by the design method used which minimize the infinity norm of the transients. However as it has been mentioned earlier, since the steady state performance are the most important, it is interesting to compare the transient behavior of those designs which achieved at least 97% of the benchmark specifications in simulation. For Level 1 the best transient performance (simulation and real-time) is achieved by Xu *et. al*. For Level 2 and 3 the best transient performance (simulation and real-time) is achieved by Wu *et. al*. To a large extent these results are not surprising since both groups use a *direct adaptive* scheme.

IX. Evaluation of the complexity

For complexity evaluation, the measure of the *Task Execution Time* (TET) in the xPC Target environment will be used. This is the time required to perform all the calculations on the

host target PC for each method. Such process has to be done on each sample time. The more complex is the approach, the bigger is the TET. One can argue that the TET depends also on the programming of the algorithm. However this will may change the TET by a factor of 2 to 4 but not by an order of magnitude. The xPC Target MATLAB environment delivers an *average* of the TET $(ATET)$. It is however interesting to asses the TET specifically associated to the controller by subtracting from the measured TET in closed loop operation, the average TET in open loop operation.
The following criteria to compare the complexity between all the approaches are defined.

$$\Delta TET_{Simple,k} = ATET_{Simple,k} - ATET_{OL_{Simple,k}} \quad (32)$$

$$\Delta TET_{Step,k} = ATET_{Step,k} - ATET_{OL_{Step,k}} \quad (33)$$

$$\Delta TET_{Chirp,k} = ATET_{Chirp,k} - ATET_{OL_{Chirp,k}} \quad (34)$$

where $k = 1,\ldots,3$. The symbols *Simple, Step* and *Chirp* are associated respectively to Simple Step Test (application of the disturbance), Step Changes in Frequency and Chirp Changes in Frequency. The global ΔTET_k for one level is defined as the average of the above computed quantities:

$$\Delta TET_k = \frac{1}{3}\left(\Delta TET_{Simple,k} + \Delta TET_{Step,k} + \Delta TET_{Chirp,k}\right) \quad (35)$$

where $k = 1,\ldots,3$. Table VII and Figure 16 summarize the results obtained by each participant for all the levels. All the values are in microseconds. Higher values indicate higher complexity. If we set three intervals : < 5 microseconds, between 5 and 15 microseconds and over 200 microseconds, one can conclude that the lowest complexity structures for Level 1 are provided by Karimi *et al.*, Xu *et al.*, Castellanos *et al.* and Aranovskiy *et al.*, for Level 2 by Karimi *et al.*, Castellanos *et al.* and Aranovskiy *et al.* and for Level 3 by Aranovskiy *et. al* and Castellanos *et al.*. The large values of the ΔTET (over 200 microseconds) can be explained for Callafon *et al.* by the large number of parameters to adapt and for Airimitoaie *et al.* by the fact that a Bezout equation has to be solved at each sampling instant. It seems that a good compromise between good steady state performance and complexity have been provided by Castellanos *et al.*, Xu *et al.*, Wu *et al.* and Aranovskiy *et al.*.

TABLE VII
TASK EXECUTION TIME FOR ALL LEVELS AND PARTICIPANTS

Participant	ΔTET		
	L1	**L2**	**L3**
Aranovskiy *et al.*	3.71	4.18	**4.92**
Callafon *et al.*	210.68	209.90	212.62
Karimi *et al.*	**2.37**	4.08	-
Wu *et al.*	14.73	14.65	14.74
Xu *et al.*	2.96	9.11	14.27
Airimitoaie *et al.*	254.24	203.83	241.22
Castellanos *et al.*	3.26	**3.90**	5.60

X. NEW PROTOCOL TEST

The benchmark specifications have been measured under pre-specified experimental protocols in terms of: 1) values of frequencies, 2) difference in frequency between two neighbor disturbances, 3) time of application of the disturbances and 4) magnitude of the step changes in frequencies. An obvious question is: what happens if the experimental protocols are changed (but maintaining the range of operation in the frequency domain)?. Since the systems are adaptive, these changes should not have too much influence upon the results.

Only two tests have been conducted for each participant, *Simple Step Test* and *Step Changes in Frequency Test*. Only the Levels 2 and 3 of the benchmark are considered.

In the original protocol, the separation (in Hz) between the sinusoidal disturbances was 20 Hz for Level 2 and 15 Hz for Level 3. For this *new* protocol, 10 Hz of separation is considered both for Level 2 and 3. The (central) frequencies chosen are in addition non integers[7] with the following values:

- 61.5 Hz − 71.5 Hz for Level 2.
- 61.5 Hz − 71.5 Hz − 81.5 Hz for Level 3.

For *Simple Step Test*, only the central frequencies are applied while for *Step Changes in Frequencies Test*, variations of $+/-5$ Hz of the central frequencies are considered (as in the benchmark protocol, in order to compare transient results).

The application time of the first disturbance was changed from 5 seconds to 3.75 seconds for both tests, but the duration of the steps in frequencies was kept at 3 seconds, in order to be able to compare the new transient results with the previous results. The measurements defined in SectionVII and the criteria from Section VIII have been used.
Table VIII gives the summary of the results concerning tuning capabilities (steady state performances) and Figure 17 gives the corresponding graphic representation. Among the designs of Wu *et al.*, Xu *et al.*, Airitimioaie *et al.* and Castellanos *et al.* which provided the best results in simulation for the benchmark protocol it appears that the designs of Airimitoaie *et al.* and Xu *et al.* are the less sensitive to changes of the experimental protocols since they succeed to achieve a BSI of 100% (Airimitoaie *et al.* for Levels 2 and 3 and Xu *et al.* for Level 2). For these two designs the changes in real time performances with respect to the case of benchmark protocols (compare with Table III) are small and an improvement in performance is obtained. A significant loss in performance both in simulation and in real time occurs for the design of Wu *et al.* at Level 3. A possible explanation is the design considered for the central controller (they provided a single controller configuration for all the levels). The design of Castellanos *et al.* show also a important loss in performance in real-time operation for Level 3.
Table IX gives the BSItrans for the case of the new protocol. One can see that most of the designs meet the benchmark specification for maximum transient duration in real-time. However in simulation the results for Xu *et al.* show a surprising slow adaptation at Level 3 while the results in real-time are good.
Taking in account both steady state performance and transient performance one can say that some of the designs are insensitive to the change of the testing protocols (i.e. different operational conditions).

[7] In the benchmark protocols only integer values have been considered.

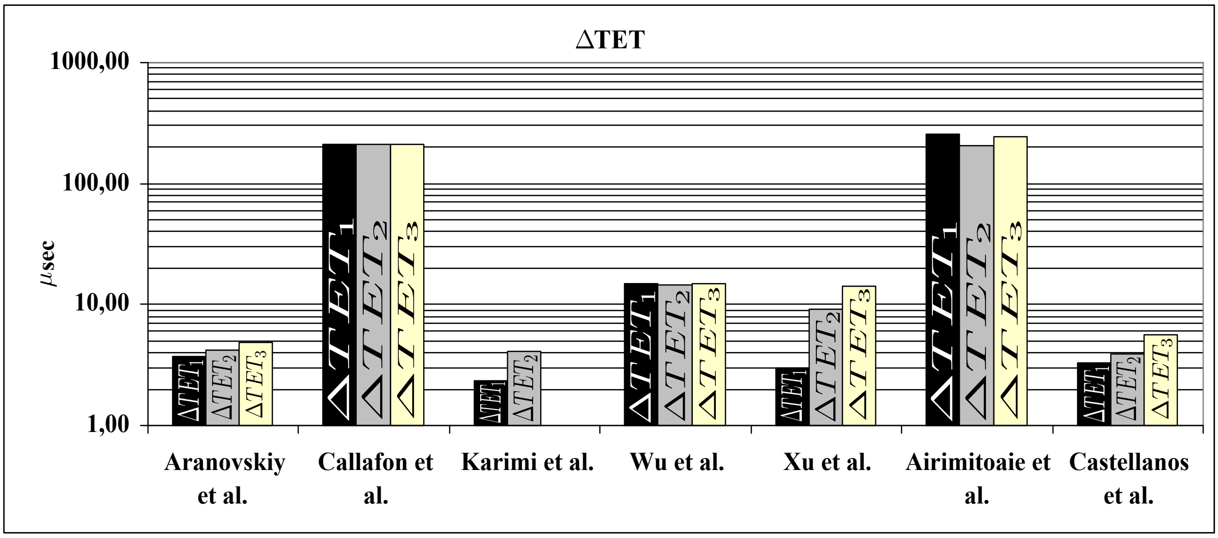

Fig. 16. The controller average task execution time (ΔTET) for all the participants.

TABLE VIII
BENCHMARK SATISFACTION INDEX FOR ALL THE PARTICIPANTS FOR THE NEW PROTOCOL

Participant	LEVEL 2				LEVEL 3			
	Simulation		**Real Time**		**Simulation**		**Real Time**	
	J_{SS_2}	BSI$_2$	J_{SS_2}	BSI$_2$	J_{SS_3}	BSI$_3$	J_{SS_3}	BSI$_3$
Aranovskiy *et al.*	4.55	57.78%	8.52	44.65%	5.26	61.62%	15.55	20.92%
Callafon *et al.*	3.33	79.95%	16.75	14.55%	5.56	65.68%	16.14	5.13%
Karimi *et al.*	5.39	68.76%	17.99	11.89%	-	-	-	-
Wu *et al.*	0.74	89.48%	1.68	76.00%	3.88	62.90%	33.79	0.00%
Xu *et al.*	**0.00**	**100.00%**	0.94	**86.63%**	0.81	95.96%	0.70	**95.05%**
Airimitoaie *et al.*	**0.00**	**100.00%**	**0.86**	**87.71%**	**0.00**	**100.00%**	**0.69**	**92.30%**
Castellanos *et al.*	1.01	85.57%	1.85	73.52%	1.14	87.30%	3.69	66.67%

TABLE IX
BENCHMARK SATISFACTION INDEX FOR TRANSIENT PERFORMANCE(FOR SIMPLE STEP TEST). NEW PROTOCOL

Index / Participant	**BSI$_{Trans_2}$**		**BSI$_{Trans_3}$**	
	Simulation	Real Time	Simulation	Real Time
Aranovsikiy *et al.*	100%	100%	100%	100%
Callafon *et al.*	100%	100%	100%	100%
Karimi *et al.*	100%	78.53%	-	-
Wu *et al.*	83.02%	100%	100%	100%
Xu *et al.*	100%	100%	0%	100%
Airimitoaie *et al.*	100%	100%	100%	100%
Castellanos *et al.*	100%	100%	100%	100%

XI. CONCLUSION

This benchmark has offered the opportunity to make a state of the art in the field of Adaptive Regulation for the case of rejection of multiple narrow band disturbances. It is the opinion of the organizers that the active vibration control system used as the support of this benchmark was relevant for the difficulties which can be encountered in practice (in particular the presence of very low damped complex zeros). Steady state performance, transient performance, robustness with respect to plant model uncertainties and complexity have been evaluated. This will allow potential users to select the appropriate approach taking in account theirs specific constraints.

Clearly not all the problems which can be encountered in the attenuation of multiple unknown time varying narrow band disturbances have been covered by the benchmark. Among future directions of research and benchmarking we mention the case of multiple narrow band disturbances with very small frequencies intervals between them[8] and the tuning of the active vibration control systems in the presence of variations of the plant model.

XII. APPENDIX A: COMPARISON OF ADAPTIVE ALGORITHMS USED

To summarize the adaptive algorithms used for each participant, the following notations have been considered:

- $p \in \mathbb{R}$ is the number of parameters to adapt[9].
- $q \in \mathbb{R}$ is the dimension of the observation matrix[10].
- $\hat{\theta}(t) \in \mathbb{R}_{p\times 1}$ is the vector of parameters to adapt.

[8]Less than 10% of the disturbance frequencies.
[9]For each case consider Table II in sec. VI.
[10]In order to consider a general parametrization, $q = 1$ is a special case.

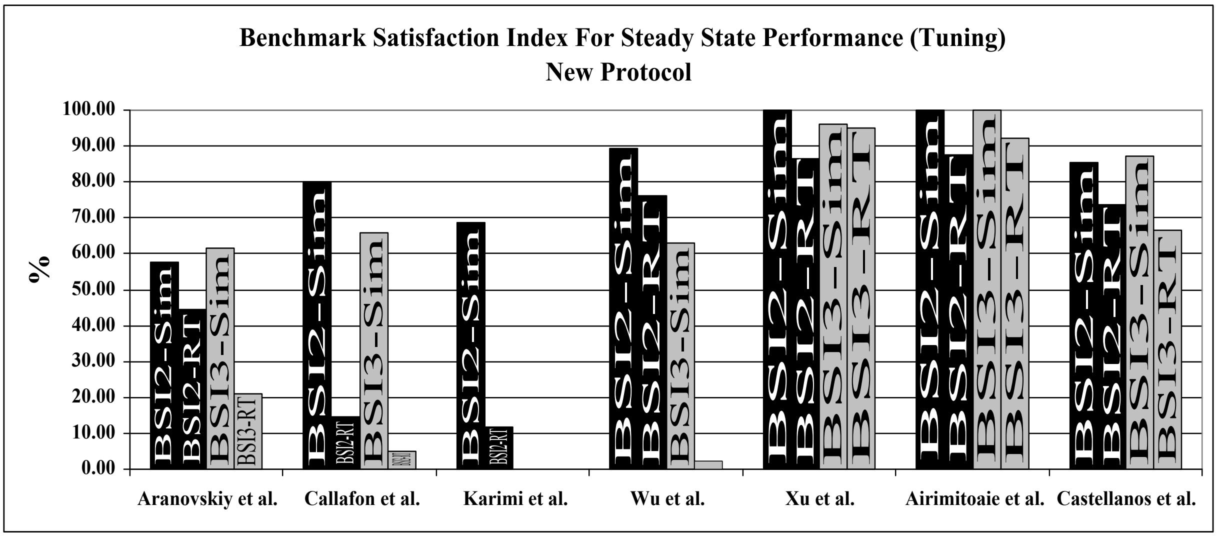

Fig. 17. Comparison of the Benchmark Satisfaction Index (*BSI*) for benchmark protocol and new protocol.

- $F(t) \in \mathbb{R}_{p\times p}$ is the adaptation matrix.
- $\Phi(t) \in \mathbb{R}_{p\times q}$ is the observation matrix.
- $\varepsilon^0(t) \in \mathbb{R}_{q\times 1}$ is the *a priori* error prediction function.
- $\zeta(t) \in \mathbb{R}_{1\times 1}$ is an auxiliary variable defined according to the participant approach.

In general all the participants use a parameter adaptation algorithm having the form:

$$\hat{\theta}(t+1) = \hat{\theta}(t) + \zeta(t)\frac{F(t)\Phi(t+1)}{1+\Phi^T(t+1)F(t)\Phi(t+1)}\varepsilon^0(t+1) \tag{36}$$

$$\varepsilon^0(t+1) = \varsigma(t+1) - \Phi^T(t+1)\hat{\theta}(t) \tag{37}$$

$$F(t+1) = \frac{1}{\lambda_1(t)}\left[F(t) - \frac{F(t)\Phi(t+1)\Phi^T(t+1)F(t)}{\frac{\lambda_1(t)}{\lambda_2(t)} + \Phi^T(t+1)F(t)\Phi(t+1)}\right] \tag{38}$$

where the parameter vector is updated using the previous value of the parameter vector and adding a correcting term which contains, the adaptation matrix, the observation matrix and the error prediction function. It is in the adaptation matrix calculations and the error prediction functions where the particularities of each contribution can be found. The error prediction function uses a signal ($\varsigma(t+1)$), which could be a disturbance prediction (as in Aranovskiy *et al.*, Karimi *et al.*, Wu *et al.* and Airimitoaie *et al.*), an input error prediction (as in Xu *et al.*), an equation error prediction (as in Castellanos *et al.*) or an output filtered prediction (as in Callafon *et al.*). This is related also to the factorization presented in section VI. Regarding the adaptation matrix, various profiles for the adaptation gains are obtained depending on the values assigned to $\lambda_1(t)$ and $\lambda_2(t)$, see details in [21]. Table X summarize the characteristics of the parameter adaptation algorithm used by each participant.

REFERENCES

[1] T. B. Airimitoaie, A. Castellanos Silva, and I. D. Landau. Indirect adaptive regulation strategy for the rejection of time varying narrow-band disturbances applied to a benchmark problem. *European Journal of Control*, 2013.

[2] F. Ben Amara, P.T. Kabamba, and A.G. Ulsoy. Adaptive sinusoidal disturbance rejection in linear discrete-time systems - Part I and 2. *Journal of Dynamic Systems Measurement and Control*, 121:648–659, 1999.

[3] S. Aranovskiy, A. Bobtsov, A. Kremlev, N. Nikolaev, and O. Slita. Identification of frequency of biased harmonic signal. *European Journal of Control*, (5):129–139, 2010.

[4] S. Aranovskiy and L. B. Freidovich. Adaptive compensation of disturbance formed as sums of sinusoidal signals with application to an active vibration control testbench. *European Journal of Control*, 2013.

[5] M. Bodson and S.C. Douglas. Adaptive algorithms for the rejection of sinusosidal disturbances with unknown frequency. *Automatica*, 33:2213–2221, 1997.

[6] X. Chen, A. Castellanos Silva, and M. Tomizuka. Adaptive model inversion for time-varying vibration rejection on an active suspension benchmark. *European Journal of Control*, 2013.

[7] X. Chen and M. Tomizuka. A minimum parameter adaptive approach for rejecting multiple narrow-band disturbances with application to hard disk drives. *IEEE Transactions on Control System Technology*, 20(2):408–415, Mar. 2012.

[8] R. A. de Callafon and H. Fang. Adaptive regulation via weigthted robust estimation and automatic controller tuning. *European Journal of Control*, 2013.

[9] Z. Ding. Global stabilization and disturbance suppression of a class of nonlinear systems with uncertain internal model. *Automatica*, 39(3):471 – 479, 2003.

[10] Z. Emedi and A. Karimi. Fixed-order lpv controller design for rejection of a sinusoidal disturbance with time-varying frequency. *2012 IEEE Multi-Conference on Systems and Control, Dubrovnik,*, 2012.

[11] T. Gouraud, M. Gugliemi, and F. Auger. Design of robust and frequency adaptive controllers for harmonic disturbance rejection in a single-phase power network. *Proceedings of the European Control Conference, Bruxelles*, 1997.

[12] G. Hillerstrom and J. Sternby. Rejection of periodic disturbances with unknown period - a frequency domain approach. *Proceedings of American Control Conference, Baltimore*, pages 1626–1631, 1994.

[13] A. Karimi and Z.Emedji. H-inf gain-scheduled controller design for rejection of time-varying narrow-band disturbances applied to a benchmark problem. *European Journal of Control*, 2013.

[14] C.E. Kinney, H.Fang, R.A. de Callafon, and M. Alma. Robust estimation and automatic controller tuning in vibration control of time varying harmonic disturbances. *Prepr. 18th IFAC World Congress,Milano, Italy*, pages 5401–5406, 2011.

[15] I. D. Landau, M. Alma, A. Constantinescu, J. J. Martinez, and M. Noe. Adaptive regulation rejection of unknown multiple narrow band disturbances (a review on algorithms and applications). *Control Engineering Practice*, 19(10):1168 – 1181, 2011.

TABLE X
PARAMETER ADAPTATION ALGORITHM

Participant	Adaptation matrix	Observation matrix (vector)	Notation
Aranovskiy *et al.*	$\zeta(t) = \frac{1+\Phi^T(t+1)F(t)\Phi(t+1)}{\lambda+\Phi^T(t+1)F(t)\Phi(t+1)}$ $\lambda_1(t) = \lambda$ $\lambda_2(t) = 1$	$\Phi(t+1) = [F_0 L\hat{p}(t+1), \cdots]^T$ $q = 1$	$\Phi(t+1) = x(t+1)$ $\hat{\theta}(t) = \hat{k}(t)$ $F(t) = P(t)$
Callafon *et al.*	$\zeta(t) = 1$ $\lambda_1(t) = 1$ $\lambda_2(t) = 1$	$\Phi(t+1) = \left[\begin{bmatrix}\gamma WD \\ N\end{bmatrix} w(t+1), \cdots\right]^T$ $q = 2$	$\Phi(t+1) = \phi(t+1)$ $\varepsilon^0(t+1) = \varepsilon(t, \hat{\theta}(t))$ $F(t) = P(t)$
Karimi *et al.*	$\zeta(t) = 1$	$\Phi(t+1) = \frac{1}{N_p}[-\hat{p}(t+1), \varepsilon(t+1), \varepsilon(t)]^T$ $q = 1$	$\Phi(t+1) = \psi_f(t+1)$ $\hat{\theta}(t) = \hat{\Theta}(t)$
Wu *et al.*	$\zeta(t) = 1$ $\lambda_1(t) = \lambda(t)$ $\lambda_2(t) = \lambda_1(t)$	$\Phi(t+1) = [T_{12}F(y(t+1) - \hat{y}(t+1)), \cdots]^T$ $q = 1$	$\Phi(t+1) = \phi(t+1)$ $\varepsilon^0(t+1) = \tilde{e}(t+1)$ $F(t) = P(t)$
Xu *et al.*	$\zeta(t) = 1$ $\lambda_1(t) = \lambda(t)$ $\lambda_2(t) = 1$	$\Phi_1(t+1) = [\psi_i(t+1), \cdots, \psi_n(t+1)]^T$ $q = 1$	$\Phi_1(t+1) = \psi(t+1)$ $F(t) = P(t)$
		$\Phi_2(t+1) = [\phi_1(t+1), \cdots, \phi_n(t+1)]^T$ $q = 1$	$\Phi_2(t+1) = \phi(t+1)$ $\varepsilon^0(t+1) = \nu^0(t+1)$ $F(t) = P(t)$
Arimitoaie *et al.*	Scalar version $\zeta(t) = 1 + \Phi^T(t+1)F(t)\Phi(t+1)$ $\lambda_1(t) = \lambda$ $\lambda_2(t) = 1$	$\Phi(t+1) = H_f \hat{p}^j(t+1)$ $q = 1$	$\Phi(t+1) = \Psi^j(t+1)$ $\hat{\theta}(t) = \hat{a}^{f_j}(t)$ $\varepsilon^0(t+1) = \varepsilon(t+1)$
Castellanos *et al.*	$\zeta(t) = 1$	$\Phi(t+1) = \frac{q^{-d}B^* H_{S_0} H_{R_0}}{P}[w(t+1), \cdots]^T$ $q = 1$	$\Phi(t+1) = \phi(t+1)$

[16] I. D. Landau, D. Rey, A. Karimi, A. Voda, and A. France. A flexible transimission system as a benchmark for robust digital control. *European Journal of Control*, 1995.

[17] I.D. Landau, M. Alma, J.J. Martinez, and G. Buche. Adaptive suppression of multiple time-varying unknown vibrations using an inertial actuator. *Control Systems Technology, IEEE Transactions on*, 19(6):1327 –1338, nov. 2011.

[18] I.D. Landau, A. Constantinescu, P. Loubat, D. Rey, and A. Franco. A methodology for the design of feedback active vibration control systems. *Proceedings of the European Control Conference 2001*, 2001. Porto, Portugal.

[19] I.D. Landau, A. Constantinescu, and D. Rey. Adaptive narrow band disturbance rejection applied to an active suspension - an internal model principle approach. *Automatica*, 41(4):563–574, 2005.

[20] I.D. Landau, R. Lozano, and M. M'Saad. *Adaptive control*. Springer, London, 1997.

[21] I.D. Landau and G. Zito. *Digital Control Systems - Design, Identification and Implementation*. Springer, London, 2005.

[22] R. Marino, G.L. Santosuosso, and P. Tomei. Robust adaptive compensation of biased sinusoidal disturbances with unknown frequency. *Automatica*, 39:1755–1761, 2003.

[23] A. Castellanos Silva, I. D. Landau, and T. B. Airimitoaie. Direct adaptive rejection of unknown time-varying narrow band disturbances applied to a benchmark problem. *European Journal of Control*, 2013.

[24] S. Valentinotti. *Adaptive Rejection of Unstable Disturbances: Application to a Fed-Batch Fermentation*. Thèse de doctorat, École Polytechnique Fédérale de Lausanne, April 2001.

[25] Z. Wu and F. Ben Amara. Youla parametrized adaptive regulation against sinusoidal exogenous inputs applied to a benchmark problem. *European Journal of Control*, 2013.